Conception and Modeling of a Novel Small Cubic Antenna Design for WSN

Gahgouh Salem[1†] , Ragad Hedi[2††] and Gharsallah Ali[3†††],

Microwave Electronics, Research Laboratory MERLAB FST, Faculty of Sciences, University El Manar, 2092, Tunis, Tunisia

Summary.
This paper presents a novel miniaturized 3-D cubic antenna for use in wireless sensor network (WSN) application. The geometry of this antenna is designed as a cube including a meander dipole antenna. A truly omnidirectional pattern is produced by this antenna in both E-plane and H-plane, which allows for non-intermittent communication that is orientation independent. The operating frequency lies in the ISM band (centered in 2.45 GHz). The dimensions of this ultra-compact cubic antenna are 1.25*1.12*1cm3 which features a length dimension λ/11. The coefficient which presents the overall antenna structure is Ka=0.44. The cubic shape of the antenna is allowing for smart packaging, as sensor equipment may be easily integrated into the cube hallow interior. The major constraint of WSN is the energy consumption. The power consumption of radio communication unit is relatively high. So it is necessary to design an antenna which improves the energy efficiency. The parameters considered in this work are the resonant frequency, return loss, efficiency, bandwidth, radiation pattern, gain and the electromagnetic field of the proposed antenna. The specificity of this geometry is that its size is relatively small with an excellent gain and efficiency compared to previously structures (reported in the literature). All results of the simulations were performed by CST Microwave Studio simulation software and validated with HFSS. We used Advanced Design System (ADS) to validate the equivalent scheme of our conception.
Input here the part of summary.

Keywords:
Wireless sensor network (WSN); Meander dipole; cubic antenna; Energy consumption; Efficiency; Size.

1. Introduction

It is well known that the use of the distributed wireless sensors network (WSN) undergoes continuous growth in the future with multiple applications such as biomedical, environmental and military monitoring. The paper aims to develop an antenna for wireless sensor node and especially for the End Devices used for embedded and through-life structural health monitoring of civil infrastructures. The importance of this design, in which applications, is to minimize the size and the power of consumption of sensor node [1]-[2] and to reach proper performance for our antenna. In a wireless sensor network, we can find two types of a node; one called Access Point (AP), and the other is an End Devices (ED) [3]. Embedding sensors nodes into natural environment or made-man object also introduces certain antenna design challenges. The aim of designing our antenna for this last (ED) is to obtain a miniaturized antenna contrary to the planar antenna which occupies the entire volume of the node. For wireless sensor node applications, most of the antennas currently in use are planar [4]-[5] due to their low-cost regarding fabrication and relatively high radiation efficiency. However, efficient planar antennas tend to give a large cross-sectional area. For this reason, we selected 3D-antenna for applications that need high-efficiency concurrently with small size, since these antennas may be of interest to produce more efficient use of the available volume by realizing relatively long antenna lengths. 3D-antennas are also advantageous in opening up the internal volume for more applications, like storage for microcontroller or batteries or other circuits. The goal of our design is to have a low-cost omnidirectional antenna that can be simply integrated into the structure packaging with the capacity to accommodate the sensor within the structure. In this paper, the design of a miniaturized, cubic antenna for use as the radiation part of an enclosed sensor in a wireless sensor node is proposed. The concept is based on meander line dipole antenna configuration [6], folded into a cube structure [7], due to the optimized positioning of the arms of the dipole and using inductive coupling matching techniques. The approach is based on the meander line dipole antenna [8] printed on two sides of the cube and connected to coaxial cable. The advantage of the use of a coaxial probe feed excitation is the direct coupling into a 50 Ω system without the need of a matching network and it's more practice concerning experimental conditions (fabrication) [9]. The simulated data prove that we can reach a good performance about their occupied volume with an excellent gain and efficiency compared to other structures described elsewhere [10].

2. Cubic antenna design

2.1 Antenna design

The arms of the dipole are usually folded to reduce the side/height dimension of the structure while sacrificing

Manuscript received February 5, 2024
Manuscript revised February 20, 2024
https://doi.org/10.22937/IJCSNS.2024.24.2.6

efficiency and bandwidth [10]. As discussed before, Genetics Algorithms may be used to guide the shape of meander line. To find the compromise between efficiency, gain and antenna size are the main subject of the present paper.

2.1 Meandered line antenna design

In this part of this paper, a meandered line half-wave dipole antenna operating at 2.45 GHz is described. The section part of the antenna is shown in Fig. 1 formed by two symmetric parts: non-meandered rectangular strips of dimensions La and Wa and two meandered components. Each of the two arms is simulated on the same side of two parallels plate of the substrate as shown in Fig.2 (a) and (b). The substrate is Roger/Duroid TMM 10i with a nominal relative dielectric constant (ξr) of 9.8 and a thickness of 1.27 millimeter. This high permittivity substrate can help to reduce the size of this antenna, although higher permittivity is unfortunately often equivalent to higher dielectric losses [11]. The meandered line technique was used to minimize the length of the arm's antenna. CST Microwave Studio simulation software was also employed to determine the total length of the meandered portion of the arms, the slot size between sections, and the number of meandered lines to minimize the antenna size without losing gain. It is desirable to have less meandering closer to the feed element where the highest concentration of current is located.

To match the input impedance close to 50 Ω, the radius of the feed and the Teflon of the cable were adjusted. In Table I, we listed the results concerning the meandered dipole antenna dimensions. The horizontal segments of the meander lines will not participate in the radiated power of the antenna because the line currents will cancel in phase each other. By leaving the meanders to be concentrated at the ends of the dipole arms so as to minimize the horizontal lengths, a larger impedance bandwidth and higher efficiency may be realized. Moreover, the use of a cubic structure in conjunction with the meander line dipole would be to investigate whether further height reduction and it could be accomplished while preserving or improving matching, efficiency and radiation characteristics. The meandered sections were rotated in a clockwise/counter-clockwise fashion and placed along z- axis as shown in Fig. 2 (a) and (b). This orientation preserves the balanced current on the dipole; when the meandered sections are not rotated with respect to each other, and the simulated radiation patterns exhibit distorted, non-dipole like characteristics. Improved gain is indeed achieved with longer non-meandered sections, requiring a compromise between antenna size and performance.

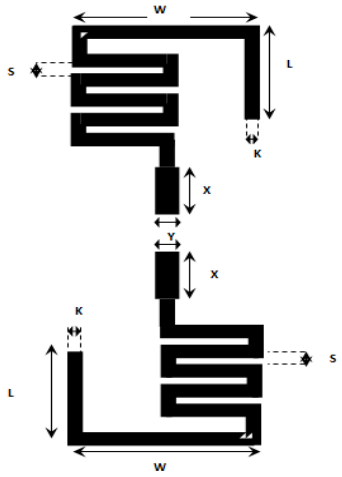

Fig.1 Planar meander line structure

Table 1. Meandered dipole antenna dimensions

Parameter	Value (mm)
y	1
X	5
W	9
L	4.5
S	0.7
K	0.8

Ka represents the overall antenna structure including the feeding network, where K=2π/λ, λ= free space wavelength, and a= radius of the smallest sphere enclosing the maximum dimension of the antenna**.**

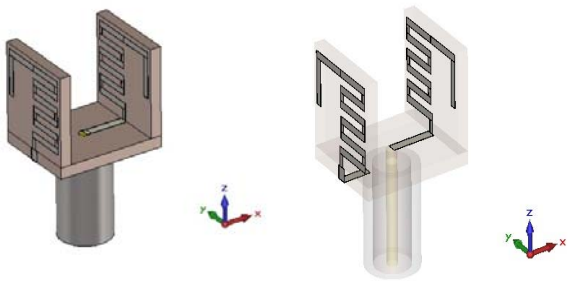

(a) (b)

Fig.2 (a) view of the cubic antenna (b) view of the meandered line integrated in the cube.

3. Results and discussion

To obtain an omnidirectional radiation pattern, an antenna dipole is a good choice. In this part, we show how to set the parameters and how to find these compromises between a good gain, a high efficiency, and a suitable miniaturization. This is the balanced triangle which is our primary goal in this work.

3.1 Return Loss

The simulated return loss S11 is shown in Fig.3. The value of the bandwidth is located at -10dB. We note that the bandwidth is not sacrificed according to data provided by the calculation. The antenna is well matched with a reflection coefficient less than -20 dB at 2.45 GHz. The resonance frequency indicates the dominant TM11 mode, and our result is validated by HFSS software.

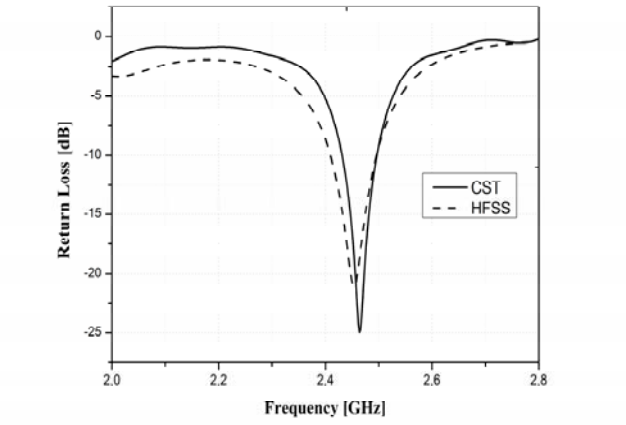

Fig. 3 simulated return-loss of the cubic antenna with CST and HFSS

3.2 Radiation pattern

The radiation pattern is almost isotropic, and it is obtained by CST Microwave Studio. No matter how the cubic wireless sensor node lands allowing for a very efficient system-on-package integration and shielding of the WSN electronics in the more spacious interior of the cube as shown in Fig.4. The gain is about 1.826 dB, and the radiation efficiency is of the order of 86% at the frequency of 2.45 GHz, as displayed in Fig.4 (a) and Fig (5). The directivity of this pattern is 2.13 dBi (simulated in CST). Figure 4 (b) shows that the HFSS simulator gives relatively the same results. In the same way, this antenna resonates at a single frequency in the North American ISM band.

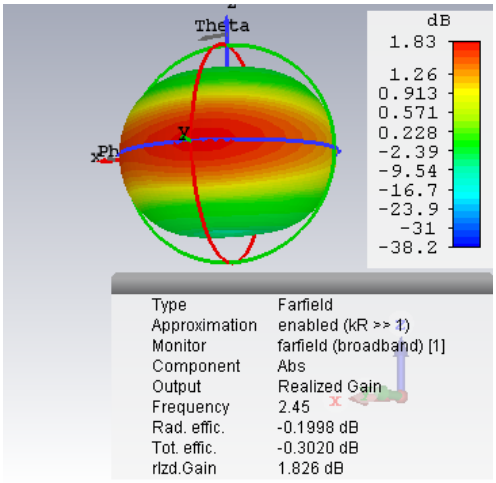

(a)

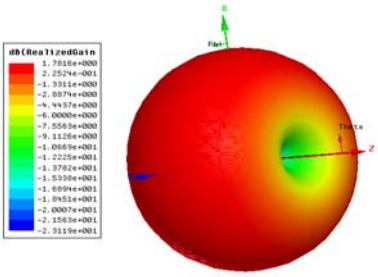

(b)

Fig. 4 3D radiation pattern in E-plan for the cubic antenna (a) CST results and (b) HFSS results.

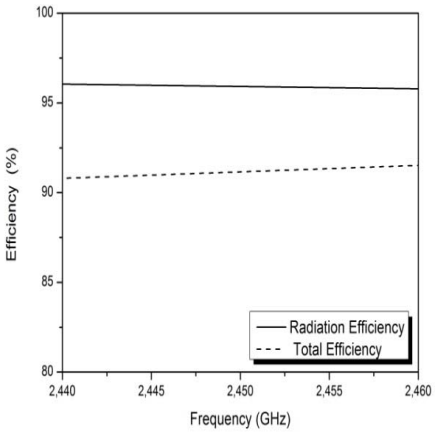

Fig. 5 Total and Radiation efficiency variation

3.3 Discussion

The table 2 summarize the comparative study results between the CST MWS and HFSS in terms of resonance frequency (fr), return loss (RL), bandwidth (BW% is calculate by equation (1)), gain, directivity and efficiency (calculated by equation (2)).

$$BW\% = \frac{2*(f_{\max} - f_{\min})}{f_{\max} + f_{\min}} \quad (1)$$

$$effeciency(\%) = \frac{Gain}{Directivity} * 100 \quad (2)$$

Table 2. Simulation results by CST and HFSS

Parameters	CST	HFSS
fr	2.45	2.449
RL	25.003	21.04
BW (%)	2.83	3.51
G (dB)	1.83	1.78
Dir (dB)	2.13	2.06
Efficiency (%)	85.9	86

There is a large correspondence between simulation results for both software. We can conclude from this table that our antenna is well defined by the narrow band (BW <4) and the important efficiency (> 86%).

4. Modeling of cubic meander antenna

Our antenna is the superposition of three parts. The first present the two microstrip lines, the second present the meander inductors of opposite direction and the third part present a parasitic capacitance (C1) which is the result of the spacing between the two menders.

Fig.6 show the equivalent electrical model (R, L, C) of the proposed antenna. Therefore, the equivalent model is calculated by using the equations (3, 4).

R1, R3, R4 and L1, L3, L4 respectively presents the resistances and inductances of a microstrip line (equation (3)) [12].

$$\begin{cases} R_{rf}(\Omega) = \dfrac{l}{w\sigma\delta(1-e^{-t/\delta})} \text{ and } \delta = \sqrt{\dfrac{2}{w\sigma\mu}} \\ L(nH) = 2*10^{-4} l \left[\ln\left(\dfrac{l}{w+t}\right) + 1.193 + \dfrac{w+t}{3l} \right] * K_g \\ K_g = 0.57 - 0.145 \ln\left(\dfrac{w}{h}\right); \dfrac{w}{h} > 0.05 \end{cases} \quad (3)$$

where: w, t, l, σ and μ present respectively the width, the thickness, the length, the conductivity and the permeability of the conductor material, h is the substrate thickness and δ is the skin depth.

The equivalent model of meander line is presented by R2 and L2 in series while parallel with a capacitor C2.

R2, L2 and C2 are calculated by equation (4) [13]-[14].

$$\begin{cases} L(\mu H) = 0.0026 a^{0.0603} L_w^{0.4429} N^{0.954} d^{0.606} w^{-0.173} \\ R_{rf}(\Omega) = \dfrac{l}{w\sigma\delta(1-e^{-t/\delta})} \text{ with } \delta = \sqrt{\dfrac{2}{w\sigma\mu}} \\ C(pF) = \dfrac{1}{\sum_{i=1}^{N} \dfrac{1}{C_i}} \text{ with } C_i = \varepsilon_0 \varepsilon_r \dfrac{L_w * L_w}{d} \end{cases} \quad (4)$$

where:
L: inductance of meander (μH)
N: number of turns
a: length of a lead (mm)
L_w: height of the meander (mm)
d: width of the meander (mm)
b: half of the height h (mm)
w: width of the printed strip (mm)
$\varepsilon_0, \varepsilon_1$: absolute and relative permittivity

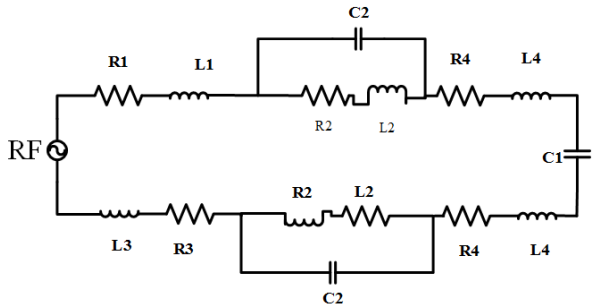

Fig. 6 Electrical model of the cubic meander antenna

To validate our model, we used the ADS schematic such as R1= R2=R3=R4=12Ohm, L1=4.8nH, L2=17.41 nH, C2=0.64pF, L3=4.3nH, C1=3.5pF. Fig 7 shows the return loss results obtained by the model validate by CST software. The resonance frequency is the equal to 2.443, return loss equal to 34 dB and BW equal to 8%. In this work, we took into account the linear model with constant values. This approximation produces an error between the theoretical expression and the electrical parameters as showin in fig.7 [15]-[16].

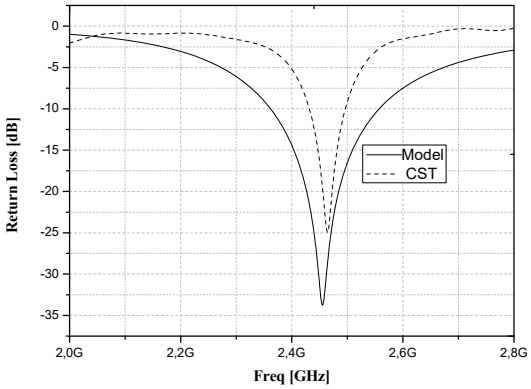

Fig. 7 Validation model

Table 3. Simulation results given by RLC model

Parameters	fr	RL	BW (%)
Value	2.443	-34	4.51

5. Immunity test for the proposed antenna

This part of the paper covers the effect of a sensor integrated into the cube. Its input impedance is readily adjusted without increasing the total occupied volume in case of modification. Fig. 7 and Figs. 8 show the influence of the block size on the antenna resonant frequency.
As seen, the dielectric blocks, with a height up to 4 mm, have little impact on the resonant frequency (0.3%<frequency shift) due to the weak coupling. The desired complex impedance can be obtained by optimizing the meandered arm parameters. This frequency shift could be accommodated by small adjustments in the antenna design. Also, the dielectric block did not affect the radiation pattern or the antenna gain.

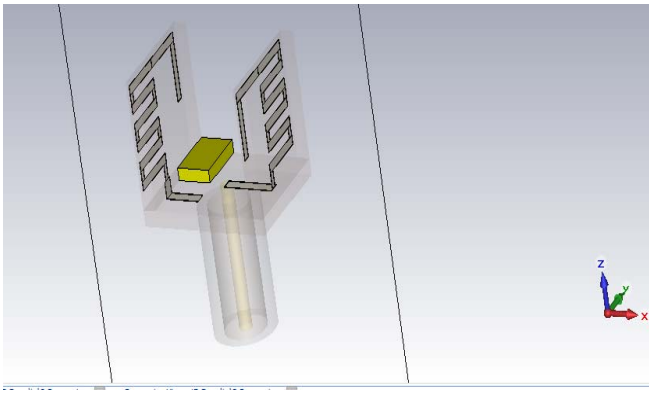

Fig. 7 Antenna and inserted block representing internal sensor electronics

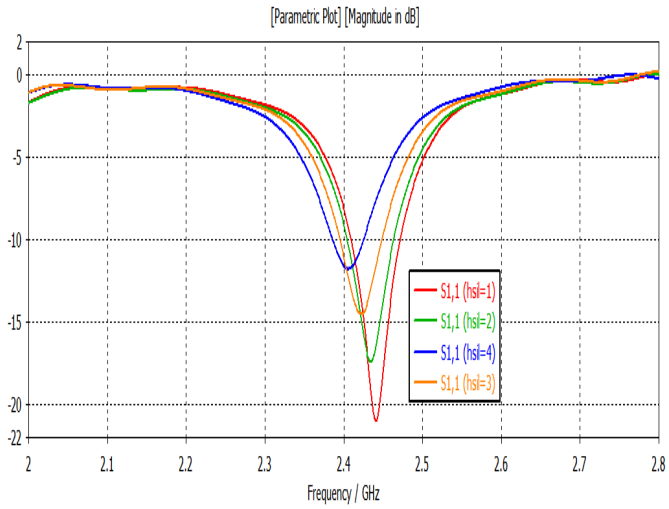

Fig. 8 Cube antenna with an inserted metallic block of different Heights

6. Conclusion

Designs of 3-D cube antenna have been developed that are good candidates to work efficiently for wireless sensor applications in narrowband where the available volume is constrained. In the first part, we showed the significance of our contribution. The performance of the antenna has been validated theoretically and confirmed to approach the theoretical performance limits for electrically small antennas. However, simulation data have proven that conductive objects, of sizes up to 5*3*2 mm³, can be placed inside the cube without significantly degrading the antenna performance and this is one more goal. Further studies are in progress to improve the performance of reconfigurable miniature antennas in frequency using active elements.

References

[1] Skiani, E. D., Mitilineos, S. A., & Thomopoulos, S. C. A., A study of the performance of wireless sensor networks operating with smart antennas. *IEEE Antennas and Propagation Magazine*, *54*(3), 50-67, (2012)

[2] Seo, J. B., On minimizing energy consumption of duty-cycled wireless sensors. *IEEE Communications Letters*, *19*(10), 1698-1701, (2015)

[3] Al Rasyid, M. U. H., Nadhori, I. U., & Alnovinda, Y. T., CO and CO 2 pollution monitoring based on wireless sensor network. In *2015 IEEE International Conference on Aerospace Electronics and Remote Sensing Technology (ICARES)* (pp. 1-5). IEEE, (2015)

[4] Herbert, S., Loh, T. H., & Wassell, I., Assessment of a low-profile planar antenna for a wireless sensor network monitoring the local water distribution network. *IET Wireless Sensor Systems*, *4*(4), 191-195, (2014)

[5] Ellis, M. S., Zhao, Z., Wu, J., Nie, Z., & Liu, Q. H., Small planar monopole ultra-wideband antenna with reduced ground plane effect. *IET Microwaves, Antennas & Propagation*, *9*(10), 1028-1034, (2015)

[6] Gahgouh, S., Ragad, H., & Gharsallah, A., Small size cubic antenna design for WSN. In *2017 18th International Conference on Sciences and Techniques of Automatic Control and Computer Engineering (STA)* (pp. 670-673). IEEE, (2017).

[7] Chiu, C. Y., & Murch, R. D., Experimental results for a MIMO cube. In *2006 IEEE Antennas and Propagation Society International Symposium* (pp. 2533-2536). IEEE, (2006)

[8] Marrocco, G., Gain-optimized self-resonant meander line antennas for RFID applications. *IEEE Antennas and Wireless propagation letters*, *2*, 302-305, (2003).

[9] Le, D. T., Huynh, T. N. T., & Nguyen, T. K., Measurements on indoor channel characteristics using wideband MIMO antennas. In *2016 3rd National Foundation for Science and Technology Development Conference on Information and Computer Science (NICS)* (pp. 44-49). IEEE, (2016)

[10] Pozar, D. M., *Microwave engineering*. John wiley & sons, (2011)

[11] Sato, Y., Campelo, F., & Igarashi, H., Meander line antenna design using an adaptive genetic algorithm. *IEEE transactions on magnetics*, *49*(5), 1889-1892, (2013)

[12] Milligan, T. A., *Modern antenna design*. John Wiley & Sons, (2005)

[13] Stojanović, G., Živanov, L., & Damjanović, M., Compact form of expressions for inductance calculation of meander inductors. *Serbian journal of electrical engineering*, *1*(3), 57-68, (2004)

[14] Bahl, I. J., *Lumped elements for RF and microwave circuits*. Artech house, (2003)

[15] Acuna, J. E., Rodriguez, J. L., & Obelleiro, F., Design of meander line inductors on printed circuit boards. *International Journal of RF and Microwave Computer-Aided Engineering: Co-sponsored by the Center for Advanced Manufacturing and Packaging of Microwave, Optical, and Digital Electronics (CAMPmode) at the University of Colorado at Boulder*, *11*(4), 219-230, (2001)

[16] Wu, R. B., Kuo, C. N., & Chang, K. K., Inductance and resistance computations for three-dimensional multiconductor interconnection structures. *IEEE Transactions on Microwave theory and Techniques*, *40*(2), 263-271, (1992)